Development of Advanced High Heat Flux Cooling System for Power Electronics

Shinmoto, Yasuhisa
Department of Aeronautics and Astronautics, Kyushu University

Miura, Shinichi
Department of Aeronautics and Astronautics, Kyushu University

Suzuki, Koichi
Department of Mechanical Engineering, Tokyo University of Science

Abe, Yoshiyuki
Department of Energy Technology Research Institute, National Institute of Advanced Industrial Science and Technology

他

出版情報：ASME 2009 InterPACK Conference. 2, pp.283-292, 2009. American Society of Mechanical Engineers : ASME
バージョン：

Proceedings of IPACK2009
InterPACK'09
July 19-23, 2009, San Francisco, California, USA

IPACK2009-89082

DEVELOPMENT OF ADVANCED HIGH HEAT FLUX COOLING SYSTEM FOR POWER ELECTRONICS

Yasuhisa Shinmoto
Department of Aeronautics and Astronautics,
Kyushu University,
Fukuoka, Japan

Shinichi Miura
Department of Aeronautics and Astronautics,
Kyushu University,
Fukuoka, Japan

Koich Suzuki
Department of Mechanical Engineering,
Tokyo University of Science,
Noda, Japan

Yoshiyuki Abe
Department of Energy Technology
Research Institute, National Institute of Advanced Industrial Science and Technology,
Tsukuba, Japan

Haruhiko Ohta
Department of Aeronautics and Astronautics,
Kyushu University,
Fukuoka, Japan

ABSTRACT

Recent development in electronic devices with increased heat dissipation requires severe cooling conditions and an efficient method for heat removal is needed for the cooling under high heat flux conditions. Most researches are concentrated on small semiconductors with high heat flux density, while almost no existing researches concerning the cooling of a large semiconductor, i.e. power electronics, with high heat generation density from a large cooling area. A narrow channel between parallel plates is one of ideal structures for the application of boiling phenomena which uses the cooling for such large semiconductors. To develop high-performance cooling systems for power electronics, experiments on increase in critical heat flux (CHF) for flow boiling in narrow channels by improved liquid supply was conducted.

To realize the cooling of large areas at extremely high heat flux under the conditions for a minimum gap size and a minimum flow rate of liquid supplied, the structure with auxiliary liquid supply was devised to prevent the extension of dry-patches underneath flattened bubbles generated in a narrow channel. The heating surface was experimented in two channels with different dimensions. The heating surfaces have the width of 30mm and the lengths of 50mm and 150mm in the flow direction. A large width of actual power electronics is realizable by the parallel installation of the same channel structure in the transverse direction. The cooling liquid is additionally supplied via sintered metal plates from the auxiliary unheated channels located at sides or behind the main heated channel. To supply the liquid to the entire heating surface, fine grooves are machined on the heating surface for enhance the spontaneous liquid supply by the aid of capillary force. The gap size of narrow channels are varied as 0.7mm, 2mm and 5mm. Distribution of liquid flow rate to the main heated channel and the auxiliary unheated channels were varied to investigate its effect on the critical heat flux. Test liquids employed are R113, FC72 and water.

The systematic experiments by using water as a test liquid were conducted. Critical heat flux values larger than $2\times10^6 W/m^2$ were obtained at both gap sizes of 2mm and 5mm for a heated length of 150mm. A very high heat transfer coefficient as much as $1\times10^5 W/m^2K$ was obtained at very high heat flux near CHF for the gap size of 2mm.

This paper is a summary of experimental results obtained in the past by the present authors.

INTRODUCTION

The quantity of semiconductor chips in an electronics device tends to increase, and they are miniaturized for dense integration. The heat generation density from the semiconductor chip has risen extremely along the increase in the processing speed. To dissipate efficiently generated heat from semiconductor chips, a heat sink consisting, for example, of metal fins, heat pipes and an air-cooling fan is used. In the cooling of semiconductors, heating surface areas of 1~ $2cm^2$ and heat generation density up to $100W/cm^2$ are often concerned as a target value, and the change of the cooling

medium from air to liquid was tried combining with the conventional cooling technology using heat spreaders. Also two-phase flow system becomes a powerful means for the cooling via the use of heat pipes. Finally, cooling devices using the phase change due to boiling and evaporation are actually investigated, and it already became a practical stage for some applications.

On the other hand, an innovative cooling technology is needed for the cooling of a large-scale semiconductors referred to as power electronics which are widely introduced in the electric power conversion process, for example, in power plants and various factories and in power controllers for hybrid automobiles. The electric power loss decreases by the low temperature operation of a new semiconductor such as SiC, which is to be introduced in place of the conventional Si semiconductors in the future. But the development of cooling technology for a large heat generation density from a large area was not yet performed in the present stage.

In space, the development of high-performance cooling system is required for the enlarged platform as a component of thermal management system. Also reduction of its size and weight is important. In the present stage, the validity of the heat transportation by two-phase flow loop system is discussed in the feasibility study of Space Solar Power System (SSPS). The technology that removes the heat from the back of the laser medium of $1m^2$ at heat flux 3×10^5– $5\times10^5 W/m^2$ which is required for the transportation of electricity to the ground or other satellites as laser power in the system of laser-fiber SSPS [1].

As just described, the development of high heat flux cooling technology from a large area is an indispensable subject in the near future, and its accomplishment will greatly contribute to the reduction of size and weight in thermal management system for space applications and also for ground ones. The cooling system using flow boiling in the narrow channel is one of possible styles to realize the present purpose.

The narrow channel is one of ideal structures because the cooling surface area can be enlarged in a limited cold plate volume. However, when boiling is applied as a cooling medium, bubble behaviors are quite different from those without the confinement of channel. In addition, flattening of generated bubbles, promotions of bubble coalescence, and reduction of quench cycle of dry-patches extended underneath bubbles are observed. Many studies of boiling heat transfer in a narrow channel were performed so far, heat transfer characteristics were clarified for different boiling system individually adopted by the researchers.

Fujita et al. [2] conducted boiling experiments by using a single rectangular narrow channel with heating surfaces of a width 30mm, lengths 30 and 120mm, and the gap size range from 0.15 to 5mm. As the narrow channel was immersed in liquid pool, the liquid velocity at the inlet of the narrow channel was varied with induced natural circulation and then with heat flux supplied. According to the experimental results of using water under the atmospheric pressure, the heat transfer coefficient took the maximum value by decreasing in the gap size of the channel, while CHF decreased monotonously. Decrease in the gap size of the channel caused the heat transfer enhancement or deterioration depending on the gap size, but caused only the reduction of CHF.

Bonjour et al. [3] conducted pool boiling experiments by using a rectangular narrow channel with a heating surface of a length 120mm and with the gap size ranging from 0.5 to 2mm. From the experimental results for R113 under the atmospheric pressure, the boiling heat transfer was more enhanced at smaller gap size in the low heat flux region.

Willingham et al. [4], simulating an array of semiconductors, performed the experiments on flow boiling by using a rectangular narrow channel on a series of nine discrete heating sections with an individual heated length of 10mm. The gap size was varied from 2 to 10mm. For FC72 under the pressure of 0.136MPa, the maximum value of CHF is obtained at the gap size of 5mm.

H. Zhang et al. [5], changed orientation of narrow channel and examined the influence on CHF. Flow boiling experiments were conducted by using the rectangular narrow channel with heating surfaces of lengths 101.6mm, width 30mm and gap size 2.5mm. At low velocities, especially for saturated conditions, CHF for downward flow was much smaller than for upward flow.

Kim et al. [6] conducted boiling experiments by using rectangular narrow channels immersed in liquid pool. The length of heating surfaces was 35mm, and the gap size was ranged from 1 to 10mm. For water under the atmospheric pressure, CHF decreased as the gap size increased when the channel inclination was in the downward-facing position (180°, horizontal), while CHF increased as the gap size became large for decreasing the inclination angle toward the vertical orientation.

As known from the above results, the heat transfer coefficient due to nucleate boiling in narrow channels can be increased with decreasing in the gap size, while CHF is decreased monotonously. The latter becomes a serious obstacle for the application of boiling phenomena to the heat transfer in narrow channels. As an extreme case, Kureta et al. [7] obtained CHF as much as $13MW/m^2$ at the gap size of 3mm for mass velocity of $7500kg/m^2s$ in flow boiling of water at atmospheric pressure for upward flow in a rectangular narrow channel. The gap size and heating surface length were varied from 0.2 to 3mm and from 50 to 200mm, respectively. In general, CHF decreases when the gap size becomes smaller and the length of heating surface becomes longer because generated vapor accumulates in the narrow channel, i.e. the occurrence of "vapor blanketing". Under these experimental conditions, burnout occurred in the subcooled region at high mass velocity and low outlet quality.

As regards the heating surface conditions Chang et al. [8] reported that the heat transfer rate became larger for rough surfaces than for flat surfaces also for boiling in narrow channels. On the effect of the gravity on flow boiling in narrow

channels between parallel plates, heat transfer characteristics were summarized by Ohta et al. [9].

As mentioned above, boiling experiments in narrow channel were conducted under various boiling systems and various conditions, but the increase in CHF was not attempted as a primarily subject except the case of super-high mass velocity. Under such situation, to challenge the increase in CHF by minimized mass velocity for flow boiling in narrow channels with a large scale heating surface becomes very important.

There are some possible methods to increase CHF values in rectangular narrow heated channels, e.g. high-subcooled boiling or microbubble emission boiling (MEB) by the application of high subcooling to inlet liquid [10], and utilizing self-wetting behaviors observed in particular mixtures where surface tension gradient due to concentration (and temperature) gradient(s) promotes the supply of liquid underneath bubbles [11]. In the current researches by the authors to cool a large scale heating surface at high heat flux, a structure of cold plates of narrow channels with auxiliary unheated channel for additional liquid supply was devised and confirmed its validity. The extensions of dry patches underneath flattened bubbles were effectively prevented by additional liquid supply from auxiliary liquid feeders. The present paper systematically summarizes a series of investigation on the relevant subject conducted so far.

This paper is a summary of experimental results obtained in the past by the present authors [12–14].

NOMENCLATURE

A_0 : nominal area of heating surface, m^2
c_{pl} : isobaric specific heat of liquid, J/kg K
G : mass velocity, kg/m^2s
h_{fg} : latent heat of vaporization, J/kg
P : pressure, Pa
q_0 : heat flux based on power input, W/m^2
q_{CHF} : critical heat flux, W/m^2
$q_{CHF,0}$: critical heat flux based on power input, W/m^2
q_w : surface heat flux, W/m^2
s : gap size of main heated channel, mm
u_{in} : inlet liquid velocity, m/s
V : volumetric flow rate, m^3/s
V_{min} : minimum volumetric liquid flow rate to evaporate all liquid at the exit of heated channel at critical heat flux, m^3/s

Greek letters

α : heat transfer coefficient, W/m^2K
$\Delta T_{sub,in}$: subcooling of inlet liquid, K
ε : performance index, -
ρ_l : liquid density, kg/m^3

subscripts

aux : based on volumetric liquid flow rate supplied to the auxiliary unheated channel
main : based on volumetric liquid flow rate supplied to the main heated channel

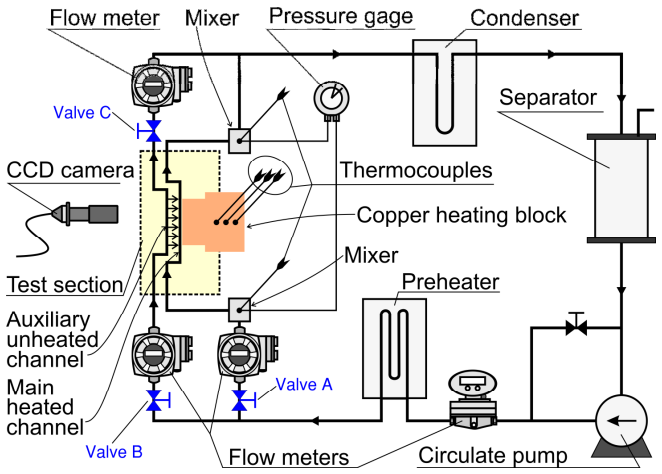

Fig. 1 Test loop.

subst : based on the sum of volumetric liquid flow rates supplied to main heated channel and from auxiliary unheated channel
suppl : based on volumetric liquid flow rate supplied from auxiliary unheated channel to main heated channel
total : based on the sum of volumetric liquid flow rates of main heated channel and auxiliary unheated channel

TEST LOOP FOR FORCED CONVECTION BOILING IN A NARROW CHANNEL

The test loop employed in the experiments on forced convection boiling for the long heated narrow channels is shown in Fig. 1. The components are similar to those in another test loop for the short heated channels. It consists of a magnet pump, flow meters, a pre-heater, a condenser, a liquid-vapor separator. Thermocouples and pressure taps are located in the mixing chambers at the inlet and the outlet of the main heated channel in order to evaluate the temperatures of bulk liquid. Distribution of flow rates to the main heated channel and to the auxiliary unheated channel is adjusted by valve at inlet of both channels. The flow meter at the exit of the auxiliary unheated channel is installed to calculate the liquid flow rate which is supplied from the auxiliary channel to the main heated channel via sintered metal plates. When the main heated channel has only outlet and the auxiliary unheated channel has only inlet, valves at inlet of the main heated channel and the outlet of auxiliary unheated channel were closed.

Local heat fluxes were evaluated from the power input to the electric heaters subtracting the heat loss by using the result of calibration. The error of the heat flux is within 3% at very high heat flux near CHF while it becomes 5% at low heat flux. The surface temperature was evaluated by the extrapolation of indicated temperature by thermocouples inserted in the copper block. The error of the surface temperature is 1K at a maximum. Flow rates of the cooling liquid were measured by Oval flow meters (Oval Co., Ltd). The error of the flow rate is within 3%.

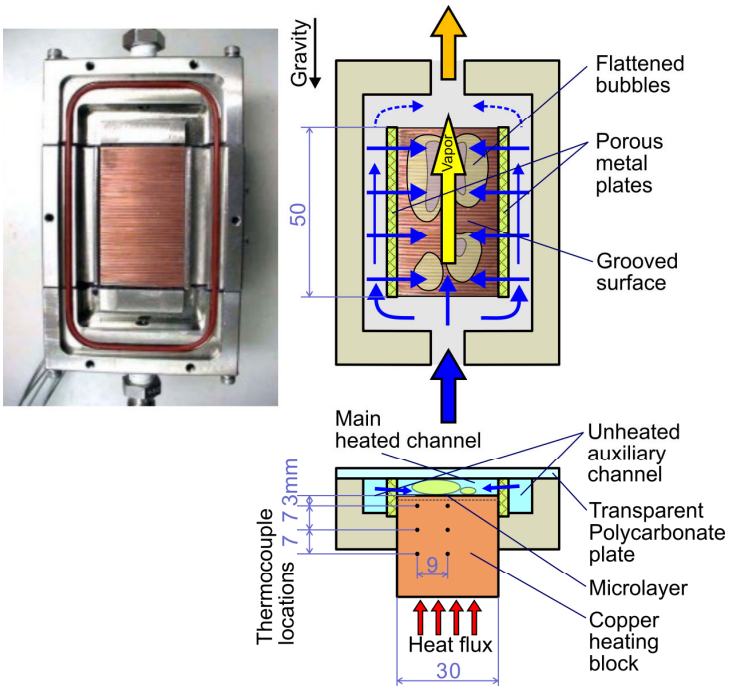

Fig. 2 Structure of grooved surface in a narrow gap with auxiliary liquid feeders (Short length 50mm).

EXPERIMENTS ON A SHORT HEATED CHANNEL FOR IMPROVED LIQUID SUPPLY

Structure of Short Heated Narrow Channel

Figure 2 shows a structure for one of the test sections employed. To increase the value of CHF, a narrow heated channel between parallel plates is modified. The main heating channel is consisted of a heating surface located at an edge of copper block and a thermoplastic resin (Polycarbonate) cover plate keeping a uniform gap size between them. Two auxiliary channels for additional liquid supply are located along both sides of the main channel, where porous metal plates separate the both. The porous plates prevent the penetration of the bubbles generated in the main heated channel into the auxiliary channels, while liquid is supplied from the auxiliary channels to the main channel. Fine grooves are machined on the heating surface in a transverse direction perpendicular to the flow, and liquid is supplied underneath flattened bubbles by the difference of capillary pressures in the grooves. Most part of the heating surface in the main heated channel, even though it is filled by bubbles at high heat fluxes, can be kept wetted by the enhanced liquid supply (represented by "E.L.S." in the figures of the present paper) via the combination of sintered metal plates and grooves on the heating surface. This driving force of liquid flow is enhanced at higher heat flux where flattened bubbles cover large areas of grooved heating surface and squeeze the meniscus of liquid filled in the grooves. Along a groove, the static pressure difference between the both phases increases due to the evaporation if the contact angle is not changed. Thus, the liquid is spontaneously led to the center of the heating surface by a negative pressure gradient.

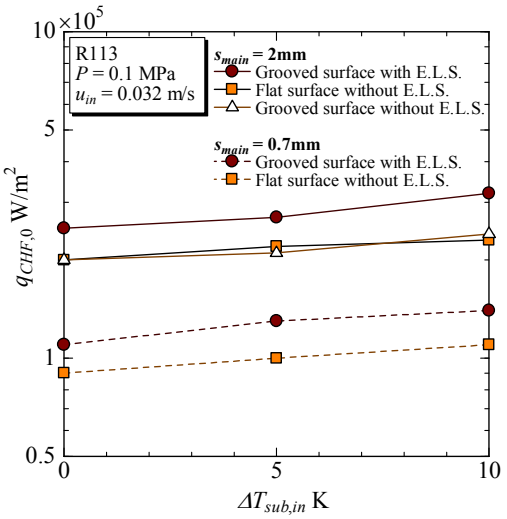

Fig. 3 Comparison of critical heat fluxes evaluated by heat input between flat and grooved surfaces (R113).

The narrow channel is vertically oriented and has a size of 30mm in width and 50mm in length in the direction of upward flow. The groove has the dimensions, 90 deg in apex angle, 1mm in depth and 2mm in pitch. The gap size between the top of the grooves and the unheated glass plate is selected as 2mm or 0.7mm. In both cases substantial mean gap size is increased to 2.5mm or 1.2mm due to the existence of grooves. Each auxiliary channel has a cross section of 6mm in width and 8mm in height.

Critical heat fluxes of R113 for Small Gaps

Figure 3 shows the relationship between CHF $q_{CHF,0}$ and inlet liquid subcooling $\Delta T_{sub,in}$ for s_{main}= 2mm and 0.7mm using R113 as test liquids with the saturation temperatures 47.6°C at P= 0.1MPa. Experiments are conducted under the inlet liquid velocity 0.032m/s (mass velocity 48kg/m^{2}s), and inlet liquid subcooling 0 – 10K. The same velocity applied to both channels. Critical heat flux is defined as the maximum value of surface heat flux q_{CHF} at the center when the heat flux corresponding to the power input q_0 is varied. The surface heat flux is evaluated based on the nominal surface area ignoring the increase of surface area due to the existence of grooves.

For u_{in}= 0.032 m/s, the followings are clarified for R113. i) At s_{main}= 2mm, $\Delta T_{sub,in}$= 0K, CHF for the flat surface is $q_{CHF,0}$= 2.0×10^5W/m^2, i.e., the same value as that calculated from Zuber correlation for pool boiling (2.0×10^5W/m^2) [14] because the conflicting effects of channel confinement and superimpose of liquid flow are cancelled. ii) For both s_{main}=2mm and 0.7mm, the effect of liquid subcooling is much smaller than the evaluation by Ivey- Morris [15], where the value of CHF is increased by 20% with the increase in the inlet liquid subcooling from 0K to 10K. From the heat balance, the

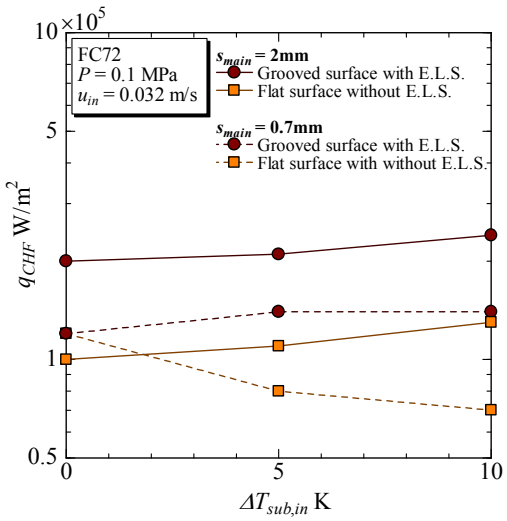

Fig. 4 Comparison of critical heat fluxes between flat and grooved surfaces (FC72).

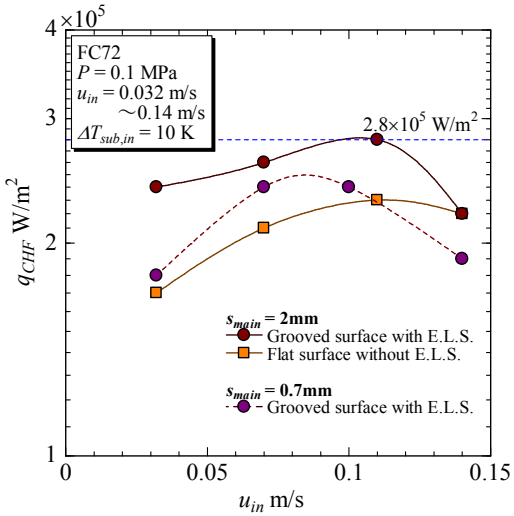

Fig. 5 Effect of inlet liquid velocity on CHF values for heating length of 50mm (FC72).

saturation state is established at the locations 4.1mm and 3.0mm, respectively for both gap sizes, from the upstream edge of the heating surface even for $\Delta T_{sub,in}$= 10K under the value of CHF shown in the figure. iii) To confirm the validity of the structure with auxiliary unheated channels, the porous metal plates for the grooved surface were replaced by plane metal plates and the supply of liquid from the auxiliary channels is prevented. The results are shown by triangle symbols in the figure. No increase of CHF values from those for the flat surface is observed, which implies that the difference in the surface roughness itself does not contribute to the increase in CHF. iv) For s_{main}= 2.0mm, CHF values for the grooved surface increased by 1.2 – 1.4 times larger than those for the flat surfaces as a result of liquid supply by the proposed structure of heating surface assembly. v) At s_{main}= 0.7mm CHF values for the grooved surface is only 1.2 – 1.3 times larger than those for the flat surface. The smaller increase in CHF than that for s_{main}= 2mm seems to be contradictory because the gap size is substantially increased by the existence of grooves especially for the present small gap size.

In the practical applications, the heating surface area is evaluated ignoring the increase of surface area by the groove structure. Then, the increase of CHF defined by the nominal area has the significance despite that no substantial increase of CHF would be expected by taking the increase of actual surface area into consideration. To find explanations for this small increase of $q_{CHF,0}$ heat flux distribution in the copper block is analyzed by using the measured values of temperatures in the block and appropriate boundary conditions.

Critical heat fluxes of FC72 for Small Gaps

Figure 4 shows the relationship between CHF q_{CHF}, i.e. surface heat flux, and inlet liquid subcooling $\Delta T_{sub,in}$ for s_{main}= 2mm and 0.7mm using FC72 as test liquids with the saturation temperatures 55.7°C at P= 0.1MPa. Experiments are conducted under the inlet liquid velocity u_{in}= 0.032m/s (mass velocity 51kg/m^{2}s), inlet liquid subcooling $\Delta T_{sub,in}$ = 0 – 10K and average heat flux q_0= 8.0×10^4 – 3.2×10^{5}W/m^2. Conditions of CHF are detected by the temperature excursion of thermocouples inserted in the heater block. To eliminate the effect of heat loss to the auxiliary liquid channels, CHF values are regarded as the maximum surface heat flux q_{CHF} at the center when input $q_{CHF,0}$ is varied. The increment of $q_{CHF,0}$ is 2.5×10^{3}W/m^2 near CHF which directly influences the resolution of the values. Before increasing the heat flux $q_{CHF,0}$ the establishment of steady state in the temperatures in the heater block is confirmed. In the present research, all heat fluxes are defined using the nominal area ignoring the existence of the grooves.

For u_{in}= 0.032 m/s, the followings are clarified for FC72. i) For s_{main}= 2mm, q_{CHF} for the grooved surface is larger by a factor 1.8 – 1.9 than those for the flat surface regardless of $\Delta T_{sub,in}$. ii) Even at s_{main}= 0.7mm, marked increase in q_{CHF} on the grooved surface is observed under the subcooled inlet conditions. The value q_{CHF} is larger by a factor 1.7 – 2.0 at $\Delta T_{sub,in}$ = 5, 10K, respectively, while almost no increase is observed at $\Delta T_{sub,in}$= 0K. iii) For s_{main}= 0.7mm, $\Delta T_{sub,in}$= 0K, the growth rate of flattened bubble is very large resulting their vigorous motion and thus the complicated shape of bubble peripheries by the liquid penetration under the imposed liquid flow. The extension of dry patches and rewetting of them by the penetrating liquid are repeated at very high frequency under the saturated inlet conditions. Hence, the liquid supply via grooves can no longer contribute to promote the quench process. iv) For s_{main}= 0.7mm, values of q_{CHF} for the flat surface decreases with increase of $\Delta T_{sub,in}$, which is interpreted as follows: The liquid subcooling prevents the growth and detachment of flattened bubbles by the balance of evaporation rate with that of condensation at the tip located in the upstream. As a result, large dry patches are extended underneath the bubbles [9].

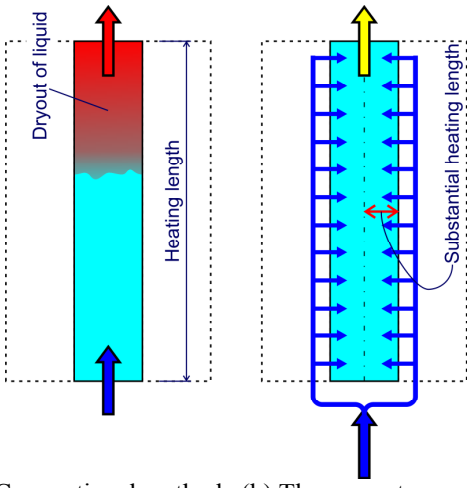

(a) Conventional method (b) The present research

Fig. 6 Difference of substantial heating length between conventional method and the present research

Effect of Inlet Liquid Velocity on Critical Heat Flux

Figure 5 shows the effect of inlet liquid velocity on CHF heating length of 50mm (FC72). The inlet liquid velocity is varied from u_{in}=0.032m/s to 0.14m/s (mass velocity 51kg/m^{2}s – 224kg/m^{2}s) under the inlet liquid subcooling of $\Delta T_{sub,in}$= 10K. It is confirmed again that at s_{main}= 2mm CHF values for the grooved surface are higher than those for the flat surface except the highest inlet liquid velocity tested. With the increase of inlet liquid velocity, CHF for the flat surface increases as expected, but the trend is saturated at higher velocity. For the grooved surface, however, maximum in CHF are clearly recognized, and further increase of inlet liquid velocity reduces CHF. At s_{main}= 2mm, the increment of CHF values by the grooved surface with the present structure disappears around the liquid velocity at 0.14m/s. The maximum in q_{CHF} is recognized also for s_{main}= 0.7mm.

The reason of the negative effect of the inlet liquid velocity on CHF is deduced as follows. At high bulk liquid velocity, flattened bubbles are separated in the transverse direction to the flow which cuts the way of liquid supply directly from the auxiliary channel to the bottom of coalesced bubbles located in the center of the heating surface. The role of grooves supplying liquid in the transverse direction becomes weaker in the presence of strong bulk flow of liquid. On the other hand, from the viewpoint of bubble behavior, the existence of grooves traps bubbles and prevents them to detach from the heating surface. In the extreme case, bulk liquid is passing over the flattened bubbles partly hidden in the grooves, which promotes the extension of dry patches underneath them. As a consequence, the area occupied by the flattened bubbles and then by dry patches on the heating surface could be larger for the grooved surface than that for the flat surface at higher liquid velocity.

EXPERIMENTS ON A LONG HEATED CHANNEL FOR ENHANCED LIQUID SUPPLY

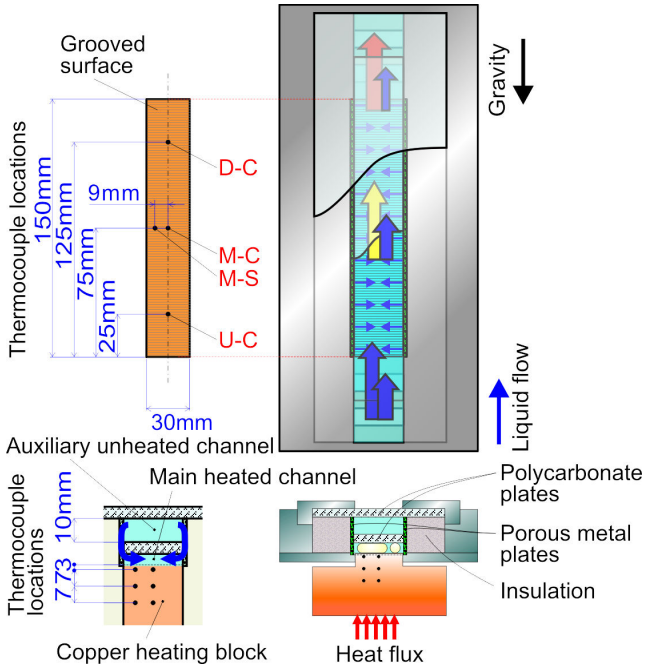

Fig. 7 A Structure of narrow heated channel assembly with auxiliary liquid supply (Long length 150mm).

Structure of Long Heated Narrow Channel

Figure 6 shows the decreasing method in substantial heating length by changing the direction of liquid supply. By this manner the substantial heated length is markedly decreased because the cooling liquid is supplied in the transverse direction perpendicular to the flow in the main heated channel. In conventional method, the dryout is caused in the downstream because of long heating length in the flow direction, while supply of sufficient liquid is possible and CHF that becomes a limitation of heat removal in nucleate boiling can be increased. Furthermore, high heat transfer coefficient can be obtained by the evaporation of thin liquid film by the grooved surface structure. In addition, the cooling for a large area is also possible by this structure arranged in parallel.

Figure 7 shows the structure of longer test section. The test section assembly has two narrow rectangular channels, i.e. a main heated channel and an auxiliary unheated channel located behind the main heated channel. The both channels are separated by a transparent plate made of polycarbonate in order to observe directly the liquid-vapor behaviors during the experiments. The main heated channel is surrounded by the boards (LOSSNA-BOARD) for thermal insulation, which prevents the indirect heat penetrations from the heating surface to the auxiliary channel. At both sides of the two channels, sintered metal porous plates with 2mm in thickness and 120μm in averaged diameter of fine holes are located through the transparent plate which divides both channels. The liquid in the auxiliary unheated channel is supplied to the main heated channel through the porous metal plates by the pressure difference between the both channels. The additional liquid

supply makes possible to keep wetted the dried areas caused by the vapor accumulation in the downstream of the main heated channel. On the heating surface, arrays of fine V-shaped grooves are machined in a transverse direction perpendicular to the bulk flow. The groove has dimensions of 0.5mm in depth and 1mm in pitch 90 deg in apex angle. The liquid is supplied underneath flattened bubbles by the difference of capillary pressures in the grooves. A heating surface with a width of 30mm and length of 150mm is realized at the end face of the heating block. By this size, a segment of an actual size of the power electronic devices of about 150mm×150mm is simulated assuming in parallel the same segment structures with 30mm width in the transverse direction.

To examine local heat transfer characteristics, four measurement points are located on the heating surface, i.e. at the distances of 25mm (Upstream–Center (U–C)), 75mm (Midstream–Center (M–C)) and 125mm (Downstream–Center (D–C)) along a center line from the bottom edge of the heating surface and at a distance of 75mm (Midstream–Side (M–S)) on the side, where thermocouples are inserted at the depth of 3mm, 10mm and 17mm at each location from the apices of grooves on the heating surface. The surface heat flux and surface temperature are evaluated from measured temperature gradients in the copper block, where both values are defined at the plane involving the apices of grooves. As in the case of the short heated channel, the surface heat flux is evaluated based on the nominal surface area ignoring the increase of surface area due to the groove structure. The heat flux was supplied from the cartridge heaters inserted in the bottom of the copper heating block.

To obtain the values of CHF, heat flux is increased in step of 1×10^5W/m^2 near the CHF and the increment becomes the resolution or accuracy of the measured values of CHF. The CHF conditions are detected by an abrupt increase of temperature, i.e. temperature excursion, at one of thermocouple locations. Before temperature excursion occurs, enough time is elapsed to obtain almost steady state conditions for all thermocouples at each heat flux level. The CHF value for each location of thermocouples is defined as the local heat flux corresponding to the power input one increment lower than the value at which the temperature excursion occurs. To avoid the damage of heating surface assembly, the heating is interrupted immediately after the temperature excursion is detected.

The experiments are conducted at near the atmospheric pressure by using water as a test fluid to achieve high CHF values because of large latent heat of vaporization. Test pressure is P= 0.13 – 0.16MPa. The gap sizes of main heated channel are s_{main}=2mm and 5mm defined as distances between the tip of grooves on the heating surface and the inner surface of unheated acrylic plate. The gap size of the auxiliary unheated channel is fixed to s_{aux}= 10mm. Experiments are performed under the conditions of inlet liquid velocity $u_{in,main}$= 0.065 – 0.2m/s for a vertical upward flow on ground and inlet liquid subcooling $\Delta T_{sub,in}$= 15K. (i)The inlet liquid velocities for the auxiliary unheated channel are varied as 1, 2/3 and 1/3 times of that for the main heated channel. (ii)The inlet liquid velocity of main heated channel $u_{in,main}$= 0m/s (Closed), outlet liquid velocity of auxiliary unheated channel $u_{out,aux}$= 0m/s (Closed). The average heat flux evaluated from the power input is q_0= $3.0\times10^5 - 3.2\times10^6$W/m^2.

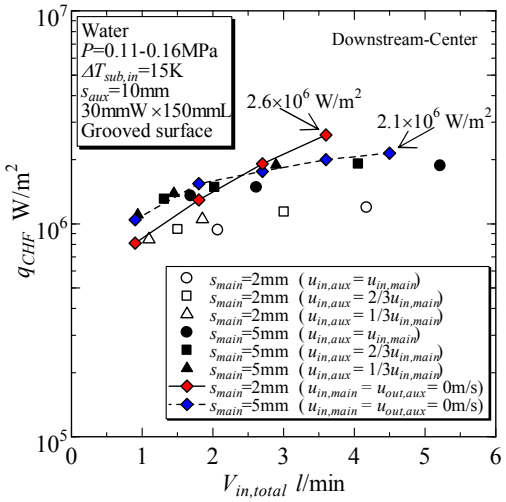

Fig. 8 Relation between CHF at downstream-center and total volumetric flow rate.

Effect of Total Volumetric Flow Rate on Critical Heat Flux

Figure 8 shows the relation between values of CHF at the downstream-center and total volumetric flow rate. When the inlet liquid velocity at the auxiliary unheated channel and the inlet liquid velocity at main heated channel are the same ($u_{in,aux}$= $u_{in,main}$), the data for s_{main}= 2mm and 5mm is shown. In the case of $u_{in,aux}$= 2/3$u_{in,main}$ and $u_{in,aux}$= 1/3$u_{in,main}$, the CHF values do not differ so much from the values for $u_{in,aux}$= $u_{in,main}$, despite of the large reduction in the liquid velocity at the inlet of auxiliary unheated channel, i.e. reduction in the total volumetric flow rate. Hence, at least for the cases of $u_{in,aux}$= $u_{in,main}$ and $u_{in,aux}$= 2/3$u_{in,main}$, additional liquid supply from the auxiliary unheated channel is excessive. In the full range of $V_{in,total}$, CHF values for s_{main}= 5mm are higher by around 1.5 times than those for s_{main}= 2mm, which indicates a large influence of gap size on CHF under the constant total volumetric flow rate conditions. When CHF values are compared at the same total volumetric flow rate $V_{in,total}$, CHF value is slightly larger in the case that the inlet liquid velocity at the auxiliary unheated channel is 2/3 or 1/3 times of the main heated channel. This result implies that slightly higher CHF values are expected if liquid flow rate to the main heated channel is increased under the restriction of the constant total volumetric flow rate. Higher values of CHF were obtained by the conditions closed inlet of the main heated channel and the auxiliary unheated channel. This result indicates the total volumetric flow rate was supplied to the main heated channel without outlet liquid of the auxiliary unheated channel.

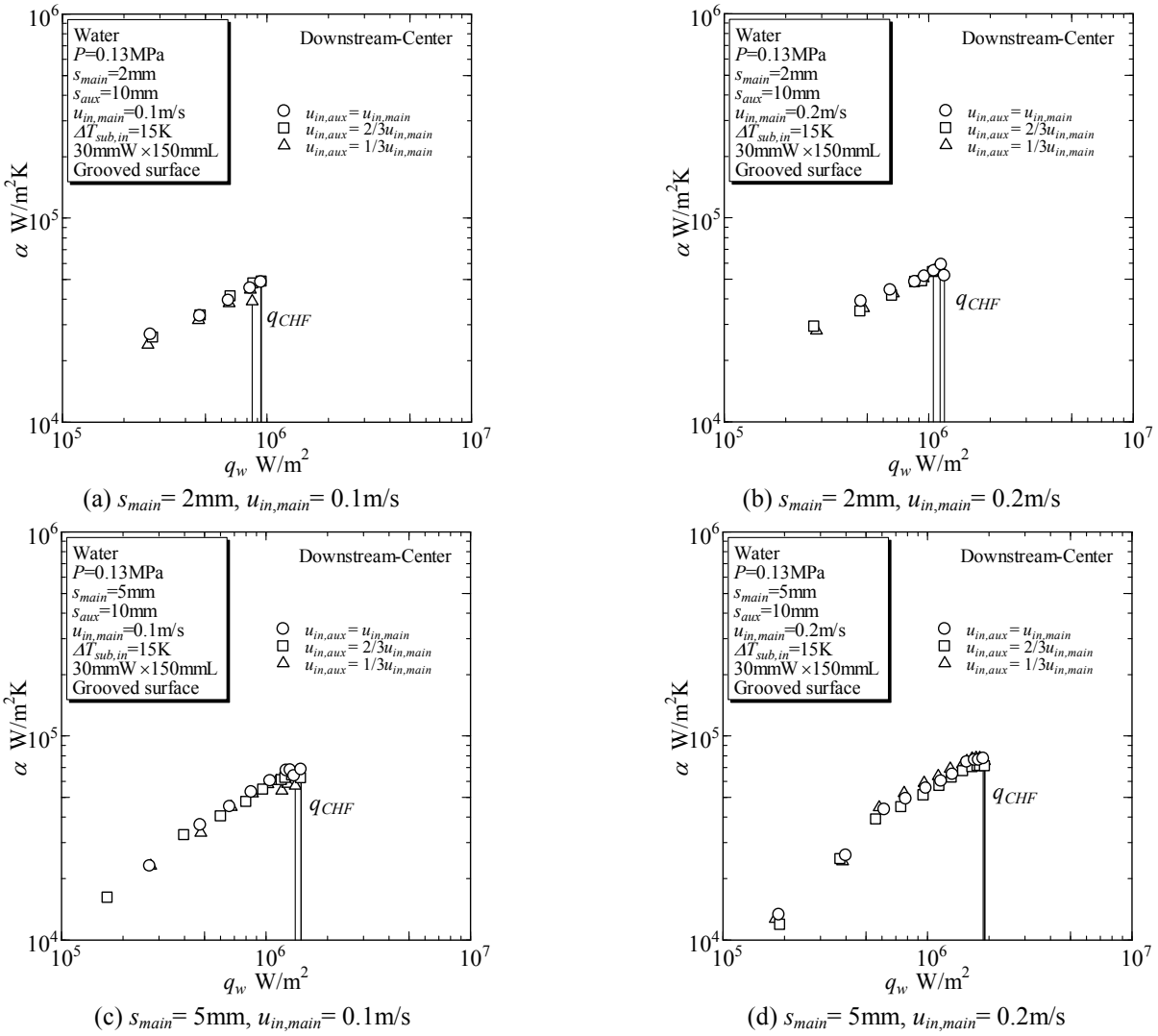

Fig. 9 Effect of inlet liquid velocity of auxiliary channel for heat transfer coefficient.

High values of CHF as much as 2×10^6W/m^2 are obtained for averaged mass velocity of 390kg/m^{2}s (3.6*l*/min as total volumetric flow rate) at the gap size of 5mm and averaged mass velocity of 720kg/m^{2}s (2.7*l*/min) at gap sizes of 2mm of main heated channel. In the several conditions, extension of dry-patches was observed at the upstream location of the main heated channel resulting the origin of burnout not from the downstream but from the upstream. It is observed that liquid is supplied to the center of heating surface by the auxiliary unheated channel located behind the main heated channel. These results were newly obtained by the conditions with a closed inlet of the main heated channel and a closed outlet of the auxiliary unheated channel.

The validity of the proposed cooling system is finally confirmed by the consideration both of flow rate and pressure drop. The liquid supply from the auxiliary channel is indispensable for the cooling system that removes heat at high heat flux from a large area. The structure requires larger pressure drop if the same total flow rate is concerned compared to the structure without auxiliary channel. The proposed structure becomes, however, more effective in the cooling of much longer surface than those tested here, where the cooling without auxiliary channel might require larger flow rate resulting the pressure drop larger than that for the structure with auxiliary channel. On the other hand, if the porous metal plates employed in the present experiments for the additional liquid supply is replaced by, for example, nozzle plates or slit plates, the pressure drop could be much smaller by the decrease in flow resistance.

Effect of Inlet Liquid Velocity on Heat Transfer Coefficients

Figure 9 shows the relationship between local heat transfer coefficient at the downstream-center and surface heat flux in the case of the gap sizes s_{main}= 2mm and 5mm, inlet liquid velocity of the main heated channel $u_{in,main}$= 0.1m/s and 0.2m/s. The data point at the right-side end implies the data just before the CHF for each condition. It is clear that deterioration of heat transfer

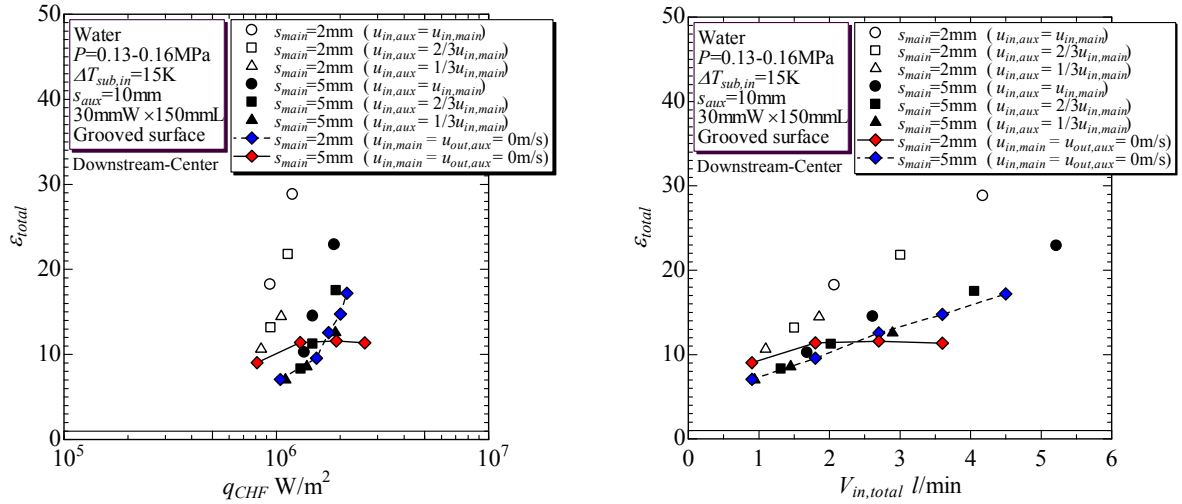

(a) Effect of critical heat flux (b) Effect of total volumetric flow rate

Fig. 10 Performance index based on the total volumetric flow rate.

coefficient does not occur by the decreasing inlet liquid velocity of auxiliary unheated channel under all conditions. In the case of s_{main}= 5mm and $u_{in,main}$= 0.2m/s, higher heat transfer coefficients as mush as 8×10^4W/m^2 is obtained just before CHF. High heat transfer coefficient is due to the evaporation of thin liquid film enhanced by the groove structure on heating surface underneath flattened bubbles. Such high heat transfer coefficients decrease required temperature difference between the surface and the cooling liquid, which becomes an important requirement for the cooling of semiconductor devices surround by atmosphere of ambient temperature. If liquid supply to the upstream can be increased by improving pressure distribution, the heat transfer coefficient becomes higher by the enhancement of thin film evaporation.

PERFORMANCE INDEX

The purpose of the present research is to realize cooling of a high heat flux from a large scale heating surface by a minimized volumetric flow rate. To evaluate the performance of cooling, an index ε is defined as follows.

$$\varepsilon = \frac{V}{V_{min}} \tag{1}$$

where, V : volumetric flow rate supplied to channel(s), m^3/s, V_{min} : minimum volumetric flow rate to evaporate all liquid at the outlet of the main heated channel under CHF, m^3/s. If the variation of inlet liquid subcooling is took into consideration, V_{min} is evaluated by

$$V_{min} = \frac{q_{CHF} A_0}{\rho_l \left(h_{fg} + c_p \Delta T_{sub,in}\right)} \tag{2}$$

where, q_{CHF} : the critical heat flux, W/m^2, A_0: the nominal area of heated surface ignoring the existence of grooves, m^2, ρ_l: liquid density, kg/m^3, h_{fg}: latent heat of vaporization, J/kg, $\Delta T_{sub,in}$: inlet liquid subcooling, K. The performance becomes higher as the value ε is lower, and ε = 1 implies complete evaporation of liquid at the exit. Hence, no excessive flow rate at ε = 1.

Figure 10 shows performance index ε_{total} defined for the total volumetric flow rate for main and auxiliary channels by the substitution of $V = V_{in,total}$ into eq.(1). As a general trend, the performance for the reduction of inlet liquid flow is higher for the structure with a closed inlet of the main heated channel and a closed outlet of the auxiliary unheated channel. In particular, this trend is remarkable for the gap size of 2mm. In the case of the structure with closed inlet of the main heated channel and closed outlet of the auxiliary unheated channel, for the gap size of 5mm, performance index increases with increasing values of CHF. Therefore the increase in the excessive liquid flow, which is not evaporated, is necessary to obtain high values of CHF. On the other hand, for the gap size of 2mm, even if values of CHF are increased, performance index tends not to increase. Then, the effective heat removal with low excessive flow is realized under the high heat flux conditions. In the case of the same total volumetric flow rate is concerned, the cooling system using a gap size of 2mm reduces the excessive liquid supply at high volumetric liquid flow rate.

CONCLUSIONS

Experiments on flow boiling in the narrow rectangular channels with a devised structure were performed to develop high-performance cooling devices for a large heat generation area like power electronics at extremely high heat flux. V-shaped grooves are machined on the heating surface in the transverse direction to the flow and liquid is supplied to the bottom of flattened bubbles via grooves from unheated liquid channel(s). The following results were clarified mainly for a long channel with heated length of 150mm.

i) Values of critical heat flux (CHF) are increased by using the present structure compared to those for the flat surface

in the narrow rectangular channels with the same gap size but without enhanced liquid supply.

ii) Though the inlet liquid velocity for the auxiliary unheated channel was reduced systematically by 2/3 and 1/3 of that for the main heated channel, CHF values and heat transfer coefficients remained almost unchanged. In the case of $u_{in,aux}$= (1/3)$u_{in,main}$, CHF value of 2×10^6W/m^2 and heat transfer coefficient of 8×10^4W/m^{2}K were obtained at mass velocity G= 33kg/m^{2}s for s_{main}= 5mm or at G= 82kg/m^{2}s for s_{main}= 2mm.

iii) Under the same total volumetric flow rate, values of CHF for the gap size of 5mm were around 1.5 times higher than those for the gap size of 2mm.

iv) Under several conditions, extension of dry-patches was observed at the upstream location of the main heated channel resulting the origin of burnout not from the downstream but from the upstream.

v) The performance for the reduction of inlet liquid flow is higher for the structure with a closed inlet of the main heated channel and a closed outlet of the auxiliary unheated channel. In particular, this trend is remarkable for the gap size of 2mm.

ACKNOWLEDGMENT

The experiments using a short heated channel were conducted under the program of NEDO (New Energy and Industrial Technology Development Organization) "Project of Strategic Development for Energy Conservation Technology, Project of Fundamental Technology Development for Energy Conservation, Development of Advanced High Heat Flux Cooling System for Power Electronics of the Next Generation", FY2002-2004. The experiments using a long heated channel were supported by a Grant-in-Aid for Scientific Research (B) (No.18360103: "Studies on the Clarification of Heat Transfer Characteristic for Flow Boiling in Small Channels and its Improvement", FY2006-2007) from the Japan Society for the Promotion of Science. The authors express appreciation for the financial support.

REFERENCES

[1] Ohta, H., Toyama, S., Kawasaki, H., Ohno, T. and Mori, M., 2003, "On the Feasibility of Heat Removal from Generator/Transmitter Units for Assumed 10MW Space Solar Power System by Using Two-phase Flow Loop with Latent heat Transportation", *Proc. IAF/54th Int. Aeronautical Congress*, *IAC-03-R.2.02*, CD-ROM 9 pages.

[2] Fujita, Y., Ohta, H., Uchida, S. and Nishikawa, K., 1988, "Nucleate boiling heat transfer and critical heat flux in narrow space between rectangular surfaces", *Int. J. Heat Mass Transfer*, **31**(2), pp. 229–239.

[3] Bonjour, J., Lallemand, M., 1998, "Flow patterns during boiling in a narrow space between two vertical surfaces", *Int. J. Multiphase Flow*, **24**, pp. 947–960.

[4] Willingham, T., C., Mudawar, I., 1992, "Channel height effect on forced-convection boiling and critical heat flux from a linear array of discrete heat sources", *Int. J. Heat Mass Transfer*, **35**(8), pp. 1865–1880.

[5] Zhang, H., Mudawar, I. and Hasan, M.M., 2002, "Experimental assessment of effects of body force, surface tension force, and inertia on flow boiling CHF", *Int. J. Heat and Mass Transfer*, **45**, pp. 4079–4095.

[6] Kim, Y. H., Kim, S. J., Kim, J. J., Noh, S., W., Suh, K. Y., Rempe, J. L., Cheung, F. B., Kim, S. B., 2005, "Visualization of boiling phenomena in inclined rectangular gap", *Int. J. Multiphase Flow*, **31**, pp. 618–642.

[7] Kureta, M., Akimoto, H., 2002, "Critical heat flux correlation for subcooled boiling flow in narrow channels", *Int. J. Heat and Mass Transfer*, **45**, pp. 4107–4115.

[8] Chang, S., W., Liou, T.-M., Lu, M., H., 2005, "Heat transfer of rectangular narrow channel with two opposite scale-roughened walls", *Int. J. Heat and Mass Transfer*, **48**, pp. 3921–3931.

[9] Ohta, H., Shinmoto, Y. and Matsunaga, K., 2002, "Effect of Gravity on Flow Boiling in Narrow Ducts and Enhancement of CHF Values", *Proc. 12th Int. heat Transfer Conf.*, **3**, pp. 725–730.

[10] Suzuki, K., Saitoh, H. and Matsumoto, K., 2006, "High Heat Flux Cooling by Microbubble Emission Boiling", *Microgravity Transport Processes in Fluid, Thermal, Biological and Materials Sciences*, *Annals of the New York Academy of Sciences*, **974**, pp. 364–377.

[11] Abe, Y., 2007, "Terrestrial and microgravity applications of self-rewetting fluids", *Microgravity - Science and Technology*, *Springer Netherlands*, **19**(3-4), pp. 11–12.

[12] Shinmoto, Y., Ohno, T., Ohta, H., Ogawa, O.and Shida, H., 2004, "High Heat Flux Cooling by Forced Convective Boiling in Narrow Channels", *Proc. 3rd International Symposium on Two-Phase Flow Modelling and Experimentation*, CD-ROM 8 pages.

[13] Shinmoto, Y., Ariki, K., Miura, S., Inada, Y. and Ohta, H., 2007, "Increase in Critical Heat Flux for Flow Boiling in Devised Narrow Channels with Enhanced Liquid Supply", *Proc. Sixth International Conference on Enhanced, Compact and Ultra-Compact Heat Exchangers: Science, Engineering and Technology*, pp. 425–432.

[14] Miura, S., Inada, Y., Shinmoto, Y. and Ohta, H., 2007, "Development of High Performance Cooling Devices for Space Application by Using Flow Boiling in Narrow Channels", *Proc. Interdisciplinary Transport Phenomena V: Fluid, Thermal, Biological, Materials, and Space Sciences*, ITP-07-43, pp. 7-32 – 7-39.

[15] Zuber, N., Tribus, M. and Westwater, J.W., 1961, "The hydrodynamic Crisis in Pool Boiling of Saturated and Subcooled Liquids", *Int. Developments in Heat Transfer*, *Pt II*, **27,** pp. 230–236,.

[16] Ivey, H.J. and Morris, D.J., 1962, "On the Relevance of the Vapor Liquid Exchange Mechanism for Subcooled Boiling Heat Transfer at Higher Pressure", *UK Atomic Energy Authority, AEEW-R*, 137.